Hexamethylmelamine: a Study of Solvation and Crystallisation

Manuel J. Aroney,* Trevor W. Hambley, Emilios Patsalides, and Raymond K. Pierens
School of Chemistry, University of Sydney, Sydney, New South Wales 2006, Australia
Hak-Kim Chan and Igor Gonda
Department of Pharmacy, University of Sydney, Sydney, New South Wales 2006, Australia

Dielectric, electro-optic, and spectroscopic properties of hexamethylmelamine (HMM) are examined in various solvents. The study is an extension of earlier work relating the dielectric characteristics of solvent to the habit of HMM crystals, a factor of importance to the effectiveness of pulmonary administration of this drug in the treatment of human small-cell lung carcinoma. In solution HMM is confirmed to be non-dipolar though abnormally large atomic polarisation is found. The optical polarisability anisotropy correlates with an extensively delocalised π-system involving the triazine ring and the exocyclic nitrogens. Interactions between HMM and cyclohexane, dioxane, and benzene are weak and not sterically defined—each of these solvents yields predominantly 'compact' crystal forms of HMM. In hexafluorobenzene definitive evidence is provided for strongly favoured stereospecific face-to-face HMM–C_6F_6 interactions. Needle-shaped crystals obtained from this solvent very rapidly become opaque and friable. Thermal analysis indicates an unstable 1 : 1 HMM–C_6F_6 adduct. This was confirmed by *X*-ray crystal structure determination which showed that HMM and C_6F_6 alternate in infinite columns, suggestive of a π–π interaction between the rings. The study provides an important correlation, based on experiment, between the statistically preferred HMM–C_6F_6 configuration in solution and that found for the crystalline adduct when isolated.

Gonda *et al.*[1–3] have studied the preparation and aerodynamic properties of different crystal forms of hexamethylmelamine (HMM) [2,4,6-tris(dimethylamino)-1,3,5-triazine], (**1**) a drug active against human small-cell lung carcinoma. Research on the crystal forms was motivated by the need to improve the efficacy of drug action of HMM and to gain information on the toxic potential with the direct pulmonary administration of this drug, a desirable procedure for the reduction of adverse systemic side effects. They noted that crystallisation of HMM from dipolar solvents yielded predominantly acicular crystals while mainly compact crystals were obtained from solvents with zero dipole moments. Both types have a hexagonal crystal lattice but differ in crystal habit. In a study of HMM from fifteen different solvents, Gonda *et al.*[3] have advanced an empirical correlation between the aspect ratio of HMM crystals and the polarity of the solvent used for crystallisation.

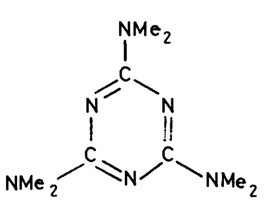

(**1**)

The present work is concerned primarily with a study of dielectric, electro-optic, and spectroscopic properties of HMM in a variety of solvents to gain some insight into the nature of intermolecular interactions in the precursor state to crystallisation. An unexpected crystal form of HMM from hexafluorobenzene led us to determine the *X*-ray structure of these crystals.

Experimental

Hexamethylmelamine was prepared and characterised as in reference 4. The solvents cyclohexane, dioxane, benzene, and hexafluorobenzene were distilled and appropriately dried over sodium or molecular sieves. Other solvents (reagent grade) were used without purification. Dielectric polarisation, microwave absorption, and electric birefringence measurements were made by techniques previously described.[5–7] Appropriate solvent constants are given in references 5 and 8. The results are summarised in Table 1. ^{1}H N.m.r. data in Table 2 were obtained on a Hitachi Perkin-Elmer R-24B n.m.r. spectrometer at 37 °C; the temperature dependence of ^{1}H n.m.r. measurements were made using a Bruker HX-90 spectrometer. Chemical shifts were extrapolated to infinite dilution, tetramethylsilane being used as internal reference.

Thermoanalytical data were obtained on a combined tga–dta instrument (Rigaku, Thermoflex M8076) using crystals of freshly filtered HMM. Hexafluorobenzene adduct HMM–C_6F_6 (7.5 mg) was heated at 10 °C min^{-1} in a stream of nitrogen (100 ml min^{-1}). Events recorded are fusion and volatilisation.

X-Ray structure determination of the HMM–C_6F_6 adduct proved very difficult since crystals of HMM–C_6F_6 are very unstable when exposed to the atmosphere, shattering and losing all crystallinity within seconds. The decomposition is evidently due to the loss of C_6F_6. To preclude this loss, various coatings were applied to the crystals but many of these absorbed the C_6F_6 leading to decomposition. Mounting in sealed capillaries also resulted in decomposition. Only a heavy coating of epoxy resin was successful in stabilizing the crystals.

Lattice parameters at 21 °C were determined by a least-square fit to the setting parameters of 25 independent reflections, measured and refined on a Enraf-Nonius CAD4F four-circle diffractometer employing graphite-monochromated Mo-K_α radiation.

Crystal Data.—$C_{15}H_{18}F_6N_6$, M_r = 396.3. Monoclinic, space group C_2/m; a = 17.631(6), b = 6.771(1), c = 15.979(3) Å,

Table 1. Molar polarisations, refractions, and molar Kerr constants of HMM in solution at T = 298 K and λ = 589.3 nm

Solvent	$\alpha\varepsilon_1$ [a]	β [a]	γ [a]	δ [a]	${}_\infty P_2/\mathrm{cm}^3$ [b]	R_D/cm^3 [b]	$10^{27}{}_\infty({}_mK_2)/\mathrm{m}^5\ \mathrm{V}^{-2}\ \mathrm{mol}^{-1}$ [c]
Cyclohexane	0.52	0.231	0.053	5.2	79 ± 2	64 ± 2	18 ± 1
Dioxane	0.65	0.007	0.137	7.35	81 ± 2	66 ± 2	21 ± 1
Benzene	0.45	0.168	0.025	0.38	77 ± 2	63 ± 2	18 ± 2
Hexafluorobenzene	0.95	−0.502	0.155	1.46	73 ± 2	61 ± 2	61 ± 2

[a] $\alpha\varepsilon_1 = \Sigma\Delta\varepsilon/\Sigma w_2$; $\beta = \Sigma\Delta d/d_1\Sigma w_2$; $\gamma = \Sigma\Delta n/n_1\Sigma w_2$; $\delta = \Sigma\Delta B/B_1\Sigma w_2$; where $\Delta\varepsilon$, Δd, Δn, and ΔB are the measured incremental changes from the pure solvent values of the relative permittivities, densities, refractive indices, and Kerr constants, respectively, for solutions having solute weight fractions w_2. [b] From symmetry the molecular electric dipole moment is zero. The difference between ${}_\infty P_2$ and R_D must be due to (field-induced) atomic polarisation of the order of 20% of R_D. [c] The solute electric birefringence is reported as ${}_\infty({}_mK_2)$, the molar Kerr constant of the solute at infinite dilution. SI units are used. The conversion factor from the electrostatic (c.g.s., e.s.u.) system is: 1 $\mathrm{m}^5\ \mathrm{V}^{-2}\ \mathrm{mol}^{-1} = 0.8998 \times 10^{15}$ e.s.u. mol^{-1}.

Table 2. Chemical shifts δ_H for protons of HMM in various solvents

Solvent	δ_H/p.p.m. [a]
C_6H_{12}	3.03
CCl_4	3.08
$CDCl_3$	3.09
C_6H_6	3.00
C_6F_6	3.05
Me_2CO	3.05
CD_3OH	3.12

[a] The precision of measurement determined from multiple runs is ±0.01 p.p.m.

Table 3. Positional parameters (× 10^4)*

	x	y	z
N(1)	6 977(10)	0	2 433(17)
C(1)	6 682(13)	0	3 226(19)
N(2)	5 912(13)	0	3 331(12)
C(2)	5 434(12)	0	2 581(13)
N(3)	5 681(10)	0	1 897(10)
C(3)	6 477(14)	0	1 847(19)
N(4)	7 091(12)	0	3 900(16)
C(4)	7 970(15)	0	3 845(18)
C(5)	6 775(14)	0	4 687(13)
N(5)	4 700(12)	0	2 709(13)
C(6)	4 376(15)	0	3 596(17)
C(7)	4 190(19)	0	1 888(26)
N(6)	6 757(11)	0	932(16)
C(8)	6 250(19)	0	224(18)
C(9)	7 496(12)	0	890(17)
F(10)	2 314(15)	0	3 087(16)
F(11)	2 211(15)	0	1 472(21)
F(12)	998(25)	0	586(25)
F(13)	−433(24)	0	1 588(28)
F(14)	−467(19)	0	3 237(26)
F(15)	1 036(20)	0	4 017(20)
C(10)	1 570(22)	0	2 893(23)
C(11)	1 558(16)	0	2 022(22)
C(12)	937(20)	0	1 463(28)
C(13)	268(27)	0	1 901(18)
C(14)	260(14)	0	2 770(17)
C(15)	893(13)	0	3 315(21)
F(10′)	7 611(30)	0	7 782(44)
F(11′)	8 454(49)	0	9 086(50)
F(12′)	10 106(60)	0	8 858(52)
F(13′)	10 613(26)	0	7 556(40)
F(14′)	9 920(29)	0	6 204(31)
F(15′)	8 469(42)	0	5 978(49)
C(10′)	1 488(49)	0	2 651(61)
C(11′)	1 214(93)	0	1 824(75)
C(12′)	581(77)	0	1 283(56)
C(13′)	565(68)	0	2 153(59)
C(14′)	835(74)	0	2 982(80)
C(15′)	1 471(74)	0	3 520(60)

* Primes indicate minor occupancy sites, occupancy = 30%.

$\beta = 91.87(3)°$, $V = 1\,906.6$ Å^3, $Z = 4$, $D_c = 1.380$ g cm^{-3}, $\mu(\text{Mo-}K_\alpha) = 1.20$ cm^{-1}, $\lambda(\text{Mo-}K_\alpha) = 0.7107$ Å, $F(000)$ 1 632 electrons.

Intensity data were collected in the range $1 < \theta < 22.5°$ using an w—θ scan. The scan width and horizontal counter apertures employed were $(1.0 + 0.35 \tan\theta)°$ and $(2.40 + 0.50 \tan\theta)$ mm, respectively. Data reduction and application of Lorentz, polarisation, and decomposition (~6%) corrections were performed using the program SUSCAD.[9] Of the 1 101 independent reflections collected, 555 with $I > 2.5\ \sigma(I)$ were considered, observed, and used in the calculations.

The structure was solved using MULTAN[10] which revealed all atoms of the HMM molecule and six atoms of the C_6F_6. All other atoms were located from subsequent difference maps.

Full-matrix least-squares refinement of an overall scale factor, positional and thermal (anisotropic for full occupancy, isotropic for disordered atoms) parameters converged (all shifts $<0.5\sigma$) with R* 0.142, R_w 0.168 and $w = 3.39/[\sigma^2(F_o) + 0.0099\ F_o{}^2]$. Maximum excursions in a final difference map were +0.5 e Å^{-3} and −0.25 e Å^{-3}. Scattering factors and anomalous dispersion terms used were those supplied in SHELX-76.[11] All calculations were carried out using SHELX-76[11] and plots were drawn using ORTEP.[12]

The atom numbering scheme is given in Figure 1. Final atomic co-ordinates are listed in Table 3.†

Discussion

Molar Kerr Constants.—From X-ray crystal structure analysis the molecule of HMM was shown to be planar (apart from the hydrogens) with D_{3h} symmetry.[13] The exocyclic carbon–nitrogen bonds are comparatively short indicating that the 'planar' configuration is stabilised through conjugation between the nitrogen lone pair electrons of the NMe_2 groups and π-orbitals of the ring. Evidence for such electron drift into the triazine ring of HMM is also found in its basic (electron-donor) character towards protons, BF_3 and trinitrobenzene.[4,14] In cyclohexane solution HMM is found to be non-dipolar (μ < 0.2 C m‡) from absence of measurable microwave absorption in the GHz region. The molar Kerr constant at infinite dilution in

---

* $R = \Sigma(|F_o| - |F_c|)/\Sigma|F_o|$, $R_w = [\Sigma w(|F_o| - |F_c|)^2/\Sigma wF_o{}^2]^{1/2}$.

† *Supplementary data* (see section 5.6.3 of Instructions for Authors in the *J. Chem. Soc., Perkin Trans. 2*, 1987, Issue 1). Lists of bond lengths and angles and of thermal parameters have been deposited at the Cambridge Crystallographic Data Centre.

‡ 1 C m = 0.2998×10^{30} D.

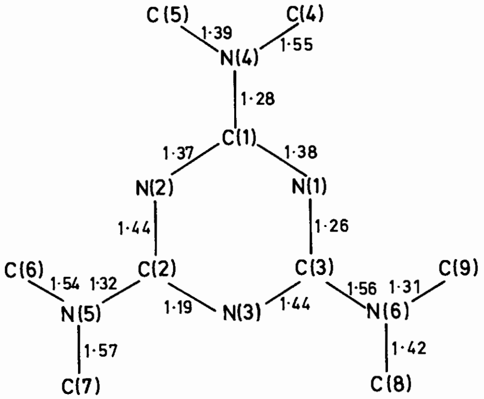

Figure 1. Atom numbering scheme of hexamethylmelamine (**1**)

cyclohexane is 18 × 10^{-27} m^5 V^{-2} mol^{-1} from which can be obtained the solute molecular optical anisotropy $\Delta b = (b_1 - b_3)$, using the Le Fèvre modified Langevin–Born expression[5]

$$_{m}K = L_{D}P(\Delta b)^2/405\,kT\varepsilon_{0E}P$$

The term b_1 (= b_2) refers to the molecular electron polarisability of HMM in the plane of the triazine ring; b_3 is the polarisability perpendicular to that plane; L, $_{D}P$ (= $_{\infty}P_2$), k, T, ε_0, and $_{E}P$ (taken as 0.95 R_D) are in turn Avogadro's number, the molar distortion polarisation, the Boltzmann constant, the absolute temperature, the permittivity of vacuum, and the molar electron polarisation. The polarisability anisotropy 10^{40} Δb* of HMM follows as 5.8 (±0.2) C m^2 V^{-1} which is somewhat greater than that of triazine 4.8 (±0.2) C m^2 V^{-1}.[15] The Δb so obtained is little affected (±0.1) if account were to be taken of the second hyperpolarisability contribution suggested for triazines by Battaglia and Richie.[15]

The effect of change of solvent environment on the molar Kerr constant has been examined. Values of the $_{\infty}(_{m}K_2)$ for HMM from solutions in cyclohexane and dioxane are quite close; the solute optical anisotropy 10^{40} Δb from dioxane is 6.3 (±0.2) C m^2 V^{-1}. Each of these solvents is non-dipolar and the solvating molecules are near isotropically polarisable. In benzene, however, it is often found that stereospecific solvation can lead to a time-averaged non-random distribution of the highly anisotropic benzene molecules about the solute and hence to a measured molar Kerr constant which is not that of the 'isolated' solute molecule but rather that of the solute–solvent cluster.[16] Such observed solvent effects on the solute $_{m}K$s have been interpreted to obtain information on the preferred stereospecific solute–solvent encounters. In the case of HMM in benzene the apparent solute $_{m}K$, and hence the molecular anisotropy of the solute together with its solvent cluster, is virtually unchanged from that in cyclohexane which means that the statistical distribution of the solvating benzene molecules is such that the solute polarisability is augmented to the same extent in the direction of the triazine plane as perpendicular to that plane. This suggests that within a dynamic cluster model, solute–solvent encounters in which the HMM and C_6H_6 planes are parallel are no more or no less favoured than encounters in which the planes are perpendicular. Steric and electrostatic considerations are used to rationalise solute–solvent interactions which are most likely to occur in a stereospecific sense at polar sites within the solute. Face-to-face approaches such as **A** in Figure 2 would result in an enhanced solute anisotropy and hence a greater apparent solute Kerr constant (in the absence of significant charge transfer). Contributions to the cluster from approaches such as **B** with the relatively electrophilic benzene periphery close to the electron-rich triazine system or to the exocyclic nitrogens would result in a decreased apparent solute Kerr constant. Angular encounters such as **C** have far less effect on the solute $_{m}K$. The effect on the solute $_{m}K$ of incoming benzenes approaching in the plane of HMM (*e.g.* **D** or **E**) would be small as their encounter with nitrogen polar centres is sterically blocked by the ring of methyl groups on the periphery of HMM. Thus no predominant HMM–benzene configuration can be identified. In hexafluorobenzene, however, the $_{\infty}(_{m}K_2)$ of HMM is 61 × 10^{-27} m^5 V^{-2} mol^{-1} clearly indicating that clustering of C_6F_6 molecules about HMM greatly augments the intrinsic solute anisotropy.[8] Thus parallel HMM–C_6F_6 configurations such as **A** would statistically be favoured. This provides direct experimental evidence to show that in the geometry of C_6F_6 solvation of HMM, **A**-type face-to-face associations are preponderant. The results correlate with intuitive argument from electrostatics as **A** represents the close approach of the π-depleted aryl system of C_6F_6 to the electron-rich triazine ring. The interactions must be weak, however, since from microwave absorption the dipole moment of HMM is *ca.* 0 in C_6F_6 solution. By contrast, perpendicular approaches such as **B** would be destabilised through repulsive interactions between negative charge centres on the plane of HMM and the fluorine atoms on the periphery of C_6F_6. Accepting **A** as the most probable encounter, the calculated $_{m}K$ for a discrete 1:1 complex HMM–C_6F_6 with this geometry is calculated to be *ca.* 52 × 10^{-27} m^5 V^{-2} mol^{-1}, a little less than the observed value. It is possible that in C_6F_6 solution associations **A** occur simultaneously above and below the plane of HMM. The data of Table 1 relate to dilute solutions but it is pertinent to note that the solute molar Kerr constants appeared to be virtually invariant with increasing solute concentration; in the case of cyclohexane this was to near saturation. Fully saturated solutions could not be studied because of the risk of precipitation in the Kerr cell and concomitant electrical discharge.

^{1}H *N.m.r. Spectra.*—^{1}H N.m.r. shifts δ_H for the HMM protons at high dilution in various solvents are shown in Table 2. Most striking is the absence of strong aromatic solvent-induced shifts which are often found with benzene and hexafluorobenzene and attributed mainly to a degree of organisation of the magnetically anisotropic C_6H_6 or C_6F_6 molecules about the sensor protons.[16,17] This lends support to the suggestion made earlier that aromatic solvent encounters with the peripheral hydrogen atoms of HMM are relatively weak and overall do not result in the preponderance of shielding or alternatively deshielding HMM–solvent configurations. This is supported also by the near constancy of the HMM proton shifts in toluene with variation of temperature (δ 2.96—2.99 for the range −50—35 °C). In the case of configuration **A** of HMM–C_6F_6 (the statistically favoured encounter from the Kerr effect analysis) the HMM protons are remote from C_6F_6 and are located between the shielding/deshielding regions of C_6F_6, thus resulting in negligibly small solvent induced changes in chemical shift. Little change in the proton shift δ was observed with increasing solute concentration up to near saturation.

Crystallisation of Hexamethylmelamine.—We find in accord with Gonda *et al.*[1–3] that predominantly needle-shaped crystals are formed from the dipolar solvents methanol, chloroform, and acetone while more equidimensional crystals tend to be obtained from cyclohexane, benzene, carbon tetrachloride,

---

* Polarisabilities are expressed in SI units throughout; the conversion factor from the c.g.s., e.s.u. system is: 1 C m^2 V^{-1} = 0.8988 × 10^{16} cm^3.

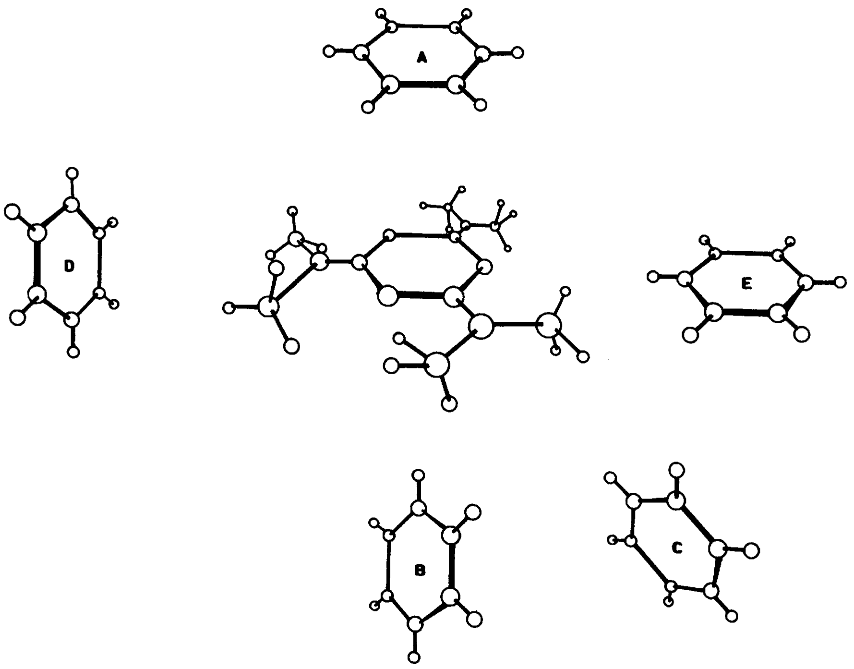

Figure 2. Stereospecific encounters between HMM and solvating aromatic molecules

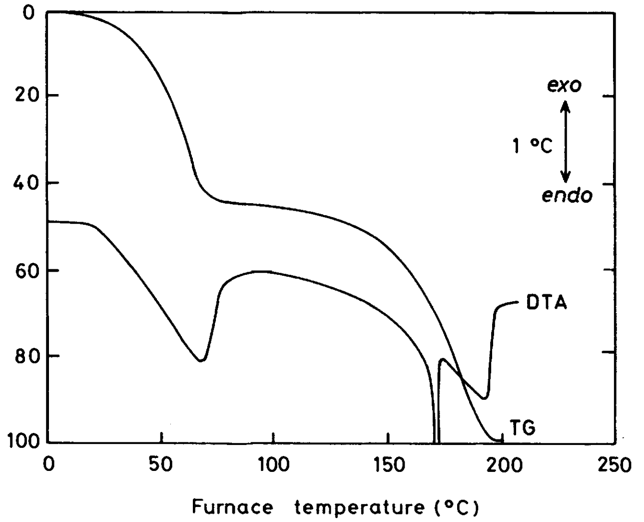

Figure 3. Thermogravimetric (TG) and differential thermal analysis (DTA) curves for the HMM–C_6F_6 adduct

and dioxane. Tetrahydropyran which resembles dioxane in geometry and in possessing a C–O–C local dipole appears to yield a mixture of crystal forms. From hexafluorobenzene are obtained long needle-shaped crystals which appears to contravene the relationship between the crystal habit and solvent polarity of reference 3 since this solvent is non-dipolar. The needles were observed to become opaque and friable within seconds of isolation from solution.

Thermal analysis was made of freshly filtered crystals of HMM from hexafluorobenzene. Thermogravimetric (TG) and differential thermal analysis (DTA) curves are shown in Figure 3. Transference of the crystals from the Buchner filter to the thermal balance was made in about 20 s by which time the surface of the crystals had become opaque. The sample was heated (10 °C min^{-1}) from room temperature to approximately 200 °C. Distinct weight changes and corresponding endothermic peaks attributed to loss of C_6F_6 were observed from room temperature to *ca.* 80 °C and for the vaporisation of HMM from 150—200 °C. A sharp endothermic peak at *ca.* 170 °C is due to fusion of HMM. The percentage weight change due to the loss of C_6F_6 was found to be *ca.* 44% compared to 47% calculated for a 1:1 HMM–C_6F_6 adduct. From this it is concluded that the precipitated HMM crystals from C_6F_6 were those of the 1:1 adduct which is similar to but much less stable than the previously known 1:1 HMM–trinitrobenzene adduct.[14]

Crystal Structure of the HMM/C_6F_6 *Adduct*.—The precision of the structure determination was severely limited by a number of factors; all crystals of the adduct obtained diffracted only weakly at higher angles and this problem was exacerbated by the need to coat the crystals with epoxy resin to preclude decomposition. Consequently a data set of limited extent was obtained restricting the type of refinement possible and making location of hydrogen atoms impossible. Secondly, the C_6F_6 molecules are severely disordered, as described below, limiting the accuracy to which they could be modelled. Accordingly, the details of the geometry of the two molecules are not discussed except to note that bond lengths obtained for HMM are in accord with those reported in more precise determinations.[13,14]

The structure consists of planar molecules lying on crystallographically imposed mirror planes at $y = 0$ and $y = \frac{1}{2}$. Molecules of HMM and C_6F_6 alternate in infinite columns parallel to the *b* axis. Thus, the separation between these molecules is equal to half the *b* cell dimension or 3.385(1) Å. Such a short contact is suggestive of a π–π interaction between the rings. Within the planes HMM and C_6F_6 alternate parallel to the *a* direction. The lines of molecules in the *a* direction are dislocated by *a*/2 with respect to each other resulting in a close packed arrangement of the columns. Closest contacts within the planes are between *N*-methyl carbon atoms and fluorine atoms

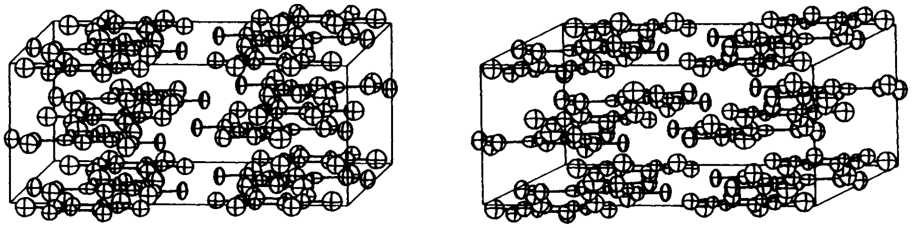

Figure 4. ORTEP View approximately, down *a* axis

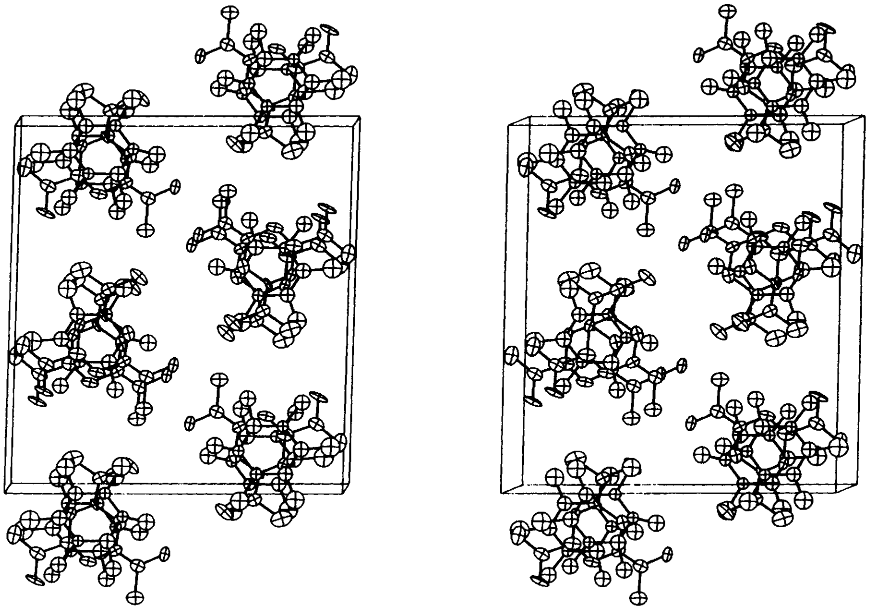

Figure 5. ORTEP View down *b* axis

in the range 2.95(4)—3.45(4) Å. The shorter of these may correspond to weak electrostatic and hydrogen-bonding attractive interactions.

The C_6F_6 molecules are rotationally disordered about the central axis. This disorder was modelled as two sites (occupancies 70:30); however, the high thermal motion of these atoms suggests that the molecule is rotating almost freely.

Conclusion

The non-dipolar nature of HMM in solution, commensurate with molecular D_{3h} symmetry from crystal structure analysis, is verified through the absence of measurable microwave absorption in the GHz region. The disparity between low- and high-frequency field polarisations is attributed to larger than usual field-induced atomic polarisations. The optical polarisability anisotropy of HMM in cyclohexane and in dioxane, derived from electric birefringence measurements, was found to be greater than that of triazine. The large 'in-plane' polarisability correlates with an extended delocalised π-system involving the triazine ring and the exocyclic nitrogens. The apparent solute electric birefringence of HMM in benzene and hence the apparent optical anisotropy of the HMM encapsulated in its benzene solvent cluster is virtually identical to that in cyclohexane. From this and concomitant ^1H n.m.r. evidence, it is inferred that HMM–C_6H_6 interactions are particularly weak and no statistically predominant stereospecific interaction can be identified. In hexafluorobenzene solution, however, the electric birefringence data provide definitive evidence for favoured face-to-face HMM–C_6F_6 encounters. Crystallisation of HMM from hexafluorobenzene yields needle-shaped crystals which very rapidly became opaque and friable. Thermal analysis indicated that the crystals so isolated are those of an unstable 1:1 HMM–C_6F_6 adduct. This was confirmed by *X*-ray crystal structure determination which showed that HMM and C_6F_6 alternate in infinite columns, suggestive of a π–π interaction between the rings. This study provides an important correlation based on experiment, between the statistically preferred HMM–C_6F_6 configuration in solution and that found for the crystalline adduct when isolated.

Acknowledgements

The authors acknowledge with gratitude a grant generously made in support of this work by the Athanase Yenibis Foundation and the award of a postgraduate scholarship by the University of Sydney to H.-K. C. as part of a URG Special Projects Grant to I. G.

References

1 I. Gonda, A. F. A. El Khalik, and A. Z. Britten, *J. Pharm. Pharmacol.* (*suppl.*), 1985, **37**, 117.

2 I. Gonda and A. F. A. P. El Khalik, Sixth International Symposium on Inhaled Particles, August 1985, Cambridge, U.K. (to be published in *Ann. Occup. Hyg.*).

3 I. Gonda, H. K. Chan, and T. Nagai, Abstract of the Annual Meeting of the Japanese Pharmaceutical Society, Chiba, Japan, 1986, vol. 25, 1.

4 S. K. Das, T. Gündüz, R. A. Shaw, and B. C. Smith, *J. Chem. Soc. A*, 1969, 1403.

5 C. G. Le Fèvre and R. J. W. Le Fèvre, in 'Techniques of Chemistry,' ed. A. Weissberger, Wiley-Interscience, New York, 1972, vol. 1, part III C, ch. 6, p. 399.

6 R. J. W. Le Fèvre, 'Dipole Moments,' Methuen, London, 1953, ch. 2.

7 S. J. Pratten, M. K. Cooper, M. J. Aroney, and S. W. Filipczuk, *J. Chem. Soc., Dalton Trans.*, 1985, 1761.

8 R. S. Armstrong, M. J. Aroney, R. K. Duffin, H. J. Stootman, and R. J. W. Le Fèvre, *J. Chem. Soc., Perkin Trans. 2*, 1973, 1362.

9 J. M. Guss, SUCAD, Data Reduction Program for the CAD4, University of Sydney, 1976.

10 G. Germain, P. Main, and M. M. Woolfson, *Acta Crystallogr., Sect. A*, 1971, **27**, 368.

11 G. M. Sheldrick, SHELX-76, A Program for *X*-ray Crystal Structure Determination, University of Cambridge, 1976.

12 C. K. Johnson, ORTEP, A Thermal Ellipsoid Plotting Program, Oak Ridge National Laboratories, Oak Ridge, 1965.

13 G. J. Bullen, D. J. Corney, and F. S. Stephens, *J. Chem. Soc., Perkin Trans. 2*, 1972, 642.

14 R. M. Williams and S. C. Wallwork, *Acta Crystallogr.*, 1966, **21**, 406.

15 M. R. Battaglia and G. L. D. Ritchie, *Mol. Phys.*, 1976, **32**, 1481.

16 R. S. Armstrong, M. J. Aroney, R. K. Duffin, H. J. Stootman, and R. J. W. Le Fèvre, *J. Chem. Soc., Perkin Trans. 2*, 1973, 1272.

17 R. D. Bertrand, R. D. Compton, and J. G. Verkade, *J. Am. Chem. Soc.*, 1970, **92**, 2702.

Received 30*th October* 1986; *Paper* 6/2107